Research Article

Journal of Environmental Nanotechnology

Seismic Performance of Reinforced Cantilever Columns in Earthquake Environments through Nano-GFRP Retrofitting

S. Venkatachalam*, K. Vishnuvardhan, V. Sampathkumar, S. S. Sugandhan, M. Rubakkumar and N. K. Surya

Department of Civil Engineering, Kongu Engineering College, Perundurai, TN, India

Received: 29.06.2024 Accepted: 25.09.2024 Published: 30.12.2024

*venkatcivil.civil@kongu.edu

ABSTRACT

The objective of this study is to evaluate the seismic behavior of reinforced concrete (RC) columns retrofitted with glass fiber reinforced polymers (GFRP). To achieve this, square RC columns measuring 1200 mm × 180 mm were cast and tested under lateral cyclic load. Two methods of wrapping, partially wrapped and fully wrapped column were used to obtain the seismic behavior of columns. Accordingly, energy absorption, stiffness, ductility, maximum bearing capacity and deformation of the specimen were examined. The glass fibers have significant impact on the results of maximum deformation; the energy absorption and stiffness of specimens wrapped with glass fiber sheets increased under seismic loads by 96% and 130%, respectively. The ductility of the specimens improved by 33% and 93% compared to conventional columns.

Keywords: GRPF; Retrofitting; Cantilever column; Seismic performance.

1. INTRODUCTION

The objective of the study is to investigate and evaluate the effectiveness of using nano glass fiber-reinforced polymer (nano-GRPF) as a retrofitting material to enhance the seismic performance of reinforced cantilever columns. This involves assessing the improvements in structural integrity and resilience of cantilever columns subjected to seismic forces when retrofitted with nano-GRPF. By analyzing the mechanical properties and behavior of the retrofitted columns under earthquake loading conditions and comparing the seismic performance of retrofitted columns to that of non-retrofitted columns, the study aims to determine the efficacy of the nano-GRPF retrofitting technique. Additionally, the study provides insights and recommendations for practical applications of nano-GRPF in seismic retrofitting of infrastructure to improve safety and durability in earthquake-prone areas. Reinforced concrete (RC) columns are crucial for the serviceability and seismic relief of multi-storied structures because they are significant vertical and lateral load-carrying components. When exposed to seismic vibrations, the columns experience the effects of axial force, shear force, and bending moment. They may fail in shear or flexure depending on the ratio of reinforcement and the aspect ratios of the RC columns (Ma and Gong, 2018). Extreme circumstances, also referred to as low-probability/high-consequence occurrences, can involve man-made disasters (such as, terrorist attacks, impacts, or explosions) or natural catastrophes (like storms, floods, and tsunamis). These occurrences frequently result in the local failure of a few structural components, which carries a risk to property and human life since it can lead to a progressive collapse. The well-known Ronan Point Apartment Block, the A.P. Murrah Federal Building, the World Trade Center Buildings, or, more recently, the Achimota Melcom Shopping Centre are a few notable events that had a significant impact on the engineering community (Adam *et al*. 2020; Kiakojouri *et al*. 2020). During an earthquake, the shear failure of a RC column can cause rapid deterioration of the column's axial load bearing capacity, lateral load capacity, and occasionally the partial or complete collapse of the structure. In order to avoid unfeasible conservatism, designers must possess the capacity to accurately assess the probability of a column collapsing under shear (Hua *et al*. 2019). Progressive collapse is the term used to describe how a breakdown spreads to additional parts until the entire structure or a disproportionately significant section of it collapses (Institute, 2006, Murray and Sasani, 2013). Important observations on the behavior of real-world buildings undergoing column shear-axial collapse are given and discussed. In Van Nuys, California, there is an RC structure called the Van Nuys Holiday Inn Building. The construction is a seven-story RC frame building with three transverse bays oriented toward the north and south and eight longitudinal bays oriented toward the east and west. The structure also includes a lofty first floor (4.11 m) (130–600) and 2.64 m (80–800) upper floors (Theiss, 2005).

Zhu *et al*. (2007) provided tools for analyzing the implied safety in the most recent ASCE 2000 rehabilitation recommendations as well as the seismic safety of existing RC structures. The main cause for concern being shear failure collapse, followed by axial column failure bearing gravity loads. Given that present code standards demand that columns in existing structures have light transverse reinforcement, that is, insufficient transverse reinforcement to avoid shear failure. A number of factors, including inadequate load-bearing capability, structural design errors, and inappropriate transverse reinforcement, can cause existing columns to be structurally defective. Reinforcement with fiber-reinforced polymer confinement is an efficient way to fortify the weak RC columns. The corner radius of the specimens and the quantity of Fiber-Reinforced Polymer (FRP) layers utilized for confinement are the primary factors influencing the efficacy of FRP (Sharma *et al*. 2013). Columns retrofitted with GFRP were investigated to determine load-carrying capability and stresses. Twenty-one 100 × 100 × 300 mm prisms were evaluated with a strain control loading. The strong constraint zone could be expanded and the stress induced zone could be reduced with a bigger radius. Therefore, a section with a corner radius was used to solve the lower confining pressure in a section caused by the generation of stresses at the edges (Benzaid *et al*. 2009). Seven specimens were tested in two groups using different codes. The tested column had the cross-section (c/s) of 305 × 305 × 914 mm. Glass fibre sheets and carbon fibre sheets were used to strengthen the column. The behaviour of the column was tested under lateral and vertical hydraulic accutators. Shear force and energy dissipation capacities of the column increased when a fiber-reinforced polymer jacket was added to the concrete cross-section. The strains in the fiber materials and transverse steel ties are reduced with an increase in the number of FRP layers (Galal *et al*. 2005). Among, tested seven columns, six specimens were tested using carbon fiber and one was tested normal. The columns were tested with seismic loading. Percentage of steel provided was under 0.1%. The test results showed more ductility (Haroun *et al*. 2002). Seven test specimens of size 200 × 200 mm were tested with carbon fiber-reinforced polymer (CFRP). The CFRP were fully wrapped continuously on two specimens and four specimens were wrapped discontinuously. The results showed more ductility on the strengthened specimens (Ye *et al*. 2002). Testing of 15 RC columns under axial compression of dimensions 125 × 125 × 1200 mm showed that GFRP wrapped columns undergo higher axial compression. Under axial load, the GFRP increased the strength and strain of the specimen. The column's ability to support an increased axial load is largely dependent on the corner radius that corresponds to the cover. The performance of the column is enhanced by adding more GFRP confinement layers (Sharma *et al*. 2013). Testing of a column measuring 305 × 305 × 1473 mm was attached to a stub measuring 508 × 762 × 813 mm in eight examples. To replicate seismic stresses, each 900-kilogram specimen was evaluated by simultaneous continuous axial and cyclic load. The findings show that further confinement using CFRP at key points improved substandard member's strength, ductility, and energy dissipation capability. A positive association was held between good behavior and increasing reinforcement layers. The behavior of similar specimens with proper lateral reinforcement was likewise outperformed by appropriately strengthened specimens (Iacobucci *et al*. 2003). A streamlined modeling approach was proposed to replicate the retrofitted FRP RC column's nonlinear cyclic behavior. The proposed model was utilized to mimic experimental testing on a bridge pier and FRP-retrofitted RC columns. Multifiber beam elements were used to achieve spatial discretization. The findings indicated that there was an improvement in strength and ductility. Additionally, the hysteretic conduct discovered numerically resembled the experimental data (Desprez *et al*. 2013). Eight short columns were examined. Their longitudinal reinforcement was higher and their transverse reinforcement was insufficient to have shear failure. Seven were strengthened with CFRP or GFRP either constantly or intermittently. The primary factor influencing the increase in damage capacity is the stiffness of the FRP reinforcement. While the reinforcement by bands causes multi-cracking around multiple rigid solids that correspond to the bands of FRP reinforcement, the fully wrapped columns exhibit the same embedded, rigid, solid behavior (Promis *et al*. 2009). Test were conducted on two low-strength poorly detailed RC columns of c/s 200 × 300 ×1250 mm under lateral cyclic loading. Low-cost GFRP were used to strengthen the specimens. Results showed the use of GFRP sheets delayed cracking and buckling of columns. The GFRP sheets enhance the seismic performance and ductility of the specimens (Yoddumrong *et al*. 2020). Eight circular columns of size 150 mm × 300 mm were subjected to compressive loading tests. 50% of the specimens had a compressive strength of 5 MPa and others with 15 MPa. The specimens were placed in one, two, and three layers of GFRP as well as being left unconfined. The specimens compressive strengths increased for one, two, and three-layer GRP wrapping, respectively, for a 5,15 MPa column as compared to the controlled specimen. The test result showed that one practical and affordable way to increase the compressive strength of low-strength concrete is to add inexpensive GFRP (Yoddumrong *et al*. 2018). When upgrading the columns of construction that uses electric devices, hemp fiber-reinforced polymer (HFRP) sheets can be put in place. Five specimens were tested under seismic loading with HFRP wraps. According to the test results, wrapping causes a slight increase in initial stiffness, but it also increases maximum strength and cracking by up to 15% since the HFRP slows down the propagation of cracks. The deformation capabilities of the specimens improve noticeably as there is more concrete confined around flexible hinge areas in the specimens covered with G

sheets (Shin and Kim, 2020). Investigations were conducted on specimens with different layers of GFRP wrap. Three control specimens and nine other specimens in total were subjected to axial compression. Every test specimen was subjected to axial compression until it broke, and its behavior in both axial and lateral directions was examined. An increased amount of GFRP wrap layers improved confinement and thus improved the column's ductility and load-bearing capability (Kumutha *et al*. 2007).

2. MATERIALS

As per IS 12269:1987, ordinary Portland cement of 53 grade was used for the experiment. M-sand with 4.75 mm sieve was used as fine aggregate. Coarse aggregate with a 20 mm sieve was used. The GFRP sheets were used as retrofitting material. To bind the sheet with the specimen, epoxy resin was used. The properties of constituent materials were determined to obtain the nominal mix design of the concrete.

3. MIX DESIGN

The specimens were cast using M20 grade of concrete. The mix was designed as per IS 10262:2009. The mix proportions were 1 (cement): 1.86 (sand): 3.32 (c. aggregate) by weight. The water/cement ratio was 0.50%.

4. SPECIMEN DETAILS

The test program consisted of three RC columns categorized into three numbers. The column has a cross-section of 180 mm × 180 mm with a length of 1200 mm. The column has its end fixed with stub support of 480 mm width and 630 mm height, as mentioned in Fig. 1. The specimens are cast using the steel mould, as shown in Fig. 2. The dimensions of the mould are the same as the specimen.

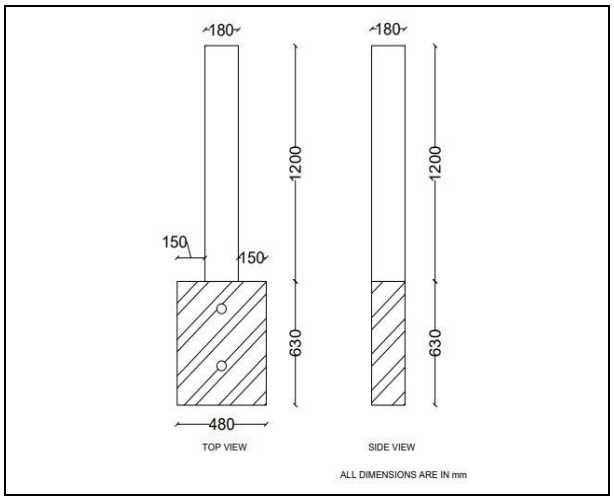

Fig. 1: Specimen dimensions

Fig. 2: Mould for specimen

4.1 Reinforcement Details

All columns are provided with four numbers of 12 mm diameter bars as main bars. The ties are provided at 150 mm center to centre with 8 mm diameter bars. The bottom support is provided with 8 mm diameter bars at 150 mm c/c at the top and bottom, as shown in Fig. 3.

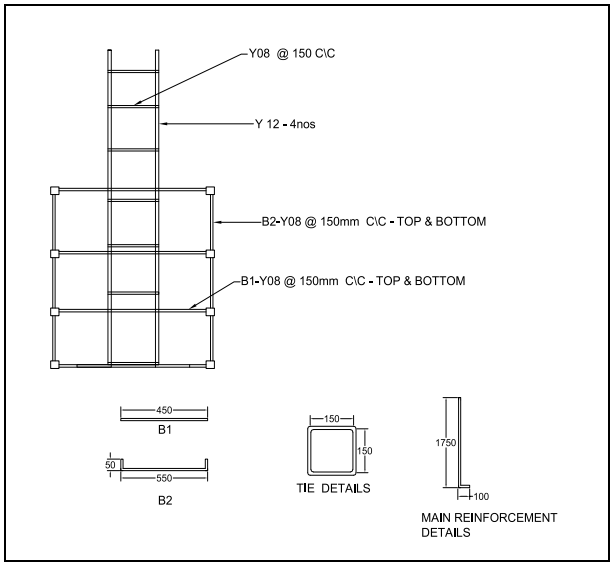

Fig. 3: Reinforcement details

5. TEST SETUP

The columns are placed at the reaction wall, as shown in Fig. 4. The actuator is fixed in the reaction wall to induce cyclic loads on the column. The LVDV are placed at the sides of the column to find the displacements occurring on the column.

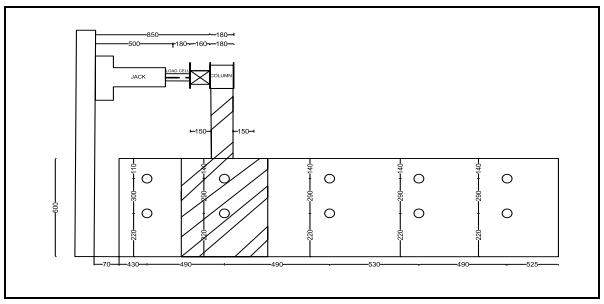

Fig. 4: Test setup of the column

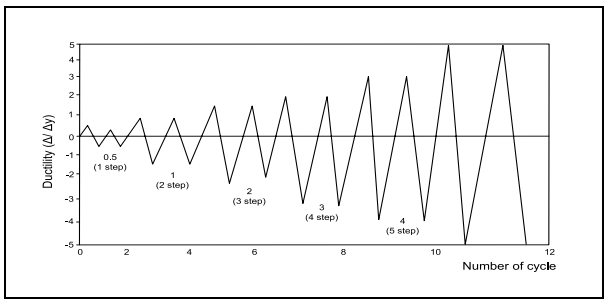

Fig. 6: Lateral displacement history (374 2013)

6. EXPERIMENTAL PROGRAM

Three columns made of RC were built with standard lateral steel finishing. Glass fiber reinforced polymer wraps were used to reinforce or repair two of these columns (Table 1). To assess the advantages of FRP retrofitting, two unwrapped columns were utilized as retrofitted specimens. Specimens retrofitted with GFRP specimens had their seismic resistance evaluated under conditions of continuous, cyclic lateral excursions that mimicked seismic stress. The key factors of the study were the behavior of GFRP retrofitted columns and the existence of column damage.

6.1 Casting of Specimens

The specimens were cast with column formwork using a ready-mixed concrete design with Portland cement, a maximum aggregate size of 20 mm, a prescribed slump of 100 mm, and a nominal compressive strength of 20 MPa. First, the stub was filled with concrete and compressed using vibrators. Afterward, the columns were cast and fully vibrated (Fig. 5). Plastic sheets were used to cover the exposed surfaces of the specimens. Additionally, three 150 ×150 mm cubes were cast alongside the column specimens to monitor the concrete's strength development over time. A water-to-cement ratio (w/c) of 0.50 was employed to ensure sufficient workability. The average compressive strength reached 13 MPa after 7 days and 18 MPa after 14 days, which is consistent with the expected concrete values.

Fig. 5: Cast specimen

6.2 Glass Fiber Reinforced Polymers (GFRP)

The chosen samples underwent retrofitting using a commercially available GFRP wrap system. The GFRP laminate utilized had an average thickness of 1.25 mm. Table 1 details the average tensile characteristics of FRP. Before the application of the FRP, the concrete surface was smoothed with sandpaper, and any voids were filled with plaster of Paris. The epoxy for the fiber wrap was formulated by combining polymer ingredients. A layer of glass fabric was laid out on a plastic sheet, cut to the required length based on the number of FRP layers in the specimen, and then coated with epoxy using a roller brush. Following the application of an epoxy coating to the column surface, the impregnated fabric was securely wrapped around the column to ensure no distortions or trapped air pockets. The GFRP was extended up to a height of 1000 mm from the stub for the column to facilitate the installation of testing instrumentation. The GFRP wraps were allowed to cure for 7 days before conducting tests on the specimens.

Table 1. Tensile properties of GFRP

Average strength, N/mm	Average rupture strain	Maximum strength, N/mm	Maximum rupture strain	Minimum strength, N/mm	Minimum rupture strain
563	0.0228	586	0.0242	540	0.0214

Table 2. Details of the test specimen

Specimen	fc′, MPa	GFRP treatment	Lateral steel	Longitudinal steel
Conventional column (CC)	22.6	None	8 mm steel at 150 mm c/c	4 numbers of 12 mm bars
Fully wrapped column (FWC)	22.8	Three layers	8 mm steel at 150 mm c/c	4 numbers of 12 mm bars
Partially wrapped column (PWC)	22.4	Three layers	8 mm steel at 150 mm c/c	4 numbers of 12 mm bars

7. TESTING OF SPECIMENS

As depicted in Fig. 4, the specimens were subjected to vertical testing within the testing frame. Table 2 provides the details of the test specimen. The applied load was measured using a load cell. Special hinges were affixed to the ends of the specimen, allowing for in-plane rotation and ensuring consistency in the loading path throughout the test. A 1000 kN load capacity actuator with a ±150 mm stroke capacity was utilized to administer reverse lateral load. Figure 5 illustrates the implementation of the actuator's displacement control function in all experiments, facilitating the application of a predetermined displacement history. To facilitate in-plane rotation at the actuator's end, modifications were made to the hinges at both ends. In accordance with engineering standards, the specimen was positioned horizontally. Plumb-bobs were utilized in the vertical plane to align the specimen with the line of action of the lateral load. Four LVDTs were employed to document the deformations at the four corners of the specimen. In cases where there was a deviation of over 5% between the average reading and the maximum or minimum displacement reading, necessary corrections were applied following the unloading of the specimen. The procedure was repeated iteratively until the material was accurately aligned. Additionally, the alignment was confirmed through measurements obtained from strain gauges. The lateral displacement sequence was applied to begin the test (Fig. 6). In this study, the cyclic loading history according to (ACI PRC-374.2-13, 2013) was used and is presented in Fig. 6. The lateral displacement cycles were repeated twice with amplitudes of 0.5Δy, 1.0Δy, 2.0y, 3.0Δy, 4.0Δy, 5.0Δy, etc. until failure, where Δy is the yield displacement evaluated assuming effective stiffness of columns (Watson and Park, 1994). The displacement was calculated using the column's theoretical section behavior and the integration of curvatures along its length. The lateral excursions were progressively increased in the following cycles until the specimen experienced its first crack at the test zone. The selected specimens earmarked for restoration experienced lateral displacement excursions, leading to the detachment of the top and bottom concrete layers. During the fifth cycle, the top and bottom concrete covers of specimen CC, subjected to lateral force, exhibited cracks. In the critical zone, the maximum displacement measured approximately 2.32 mm. The extent of damage causing concrete fracture was considered acceptable for the majority of columns identified for restoration. As a precautionary measure during the repair process, the specimen was returned to the zero lateral displacement position. During the repair, loose concrete was meticulously removed from the damaged column. A non-shrinking grout was applied to mend the fractured specimen. Once the grout had dried and set, a GFRP casing was applied and left to cure for three days. After the GFRP sheet had cured, the specimen underwent lateral load testing until failure. The same methodology of wrapping, retesting, and repairing was implemented, mirroring the approach used for Specimen PWC.

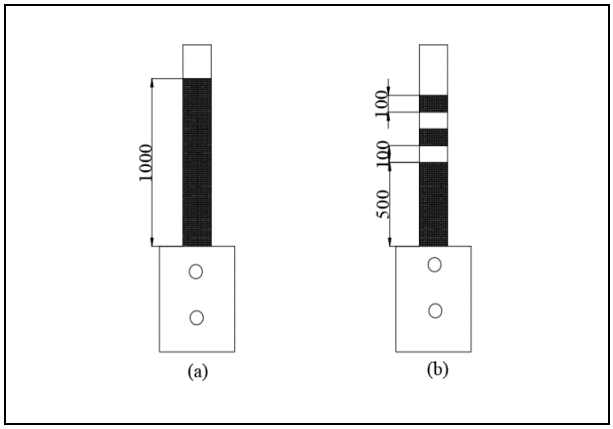

Fig. 7: (a) Fully wrapped column, and (b) Partially wrapped column

Fig. 7 (a) and 7 (b) shows fully wrapped and partially wrapped columns, respectively.

8. TEST RESULTS

8.1 Failure Modes and Observations

Cyclic loading was uniformly applied to all specimens by exerting pressure on the top edge of the column in both forward and backward directions. In specimen CC, the initial indication of distress manifested as cracks in the cover concrete along the sides of the column. Shear cracks emerged between 100 to 250 mm from the stub face during the initial three cycles, indicating a predominant influence of shear effects on the specimen's behavior. For the wrapped specimens, the initial signs of crushing and cracking in the concrete cover were not visually apparent. However, as the concrete began to fracture, the separation of fibers from the concrete, evident through a change in FRP color, became visible in all specimens within the test zones. The escalating cracking noises emanating from the hardened epoxy within the hinging zone, intensifying with lateral movements, served as an indicator of the severity of deformation. The initial sign of deformation in the successive cycles became evident through the emergence of ridges or bumps on the side surfaces of the specimens within the test region. Most of these ridges initiated between 200 and 325 mm from the point where the column contacted the stub. With increased cyclic excursions, these ridges extended in both length and height. The primary zone of damage extended from approximately 350 mm to 60 mm from the interface of the stub, characterized by audible popping noises from the cured epoxy matrix and the formation of ridges. The column section adjacent to the stub encountered the highest moment, yet the initiation of damage occurred at a comparatively weaker point on the stub, gradually progressing towards it. Prior to failure, noticeable

dilation was observed in the plastic hinge sections of all specimens during the concluding cycles. The onset of failure was marked by the lateral rupture of fibers in the last loading cycle. In specimen CC, FWC, and PWC, the sections nearest to the stub face (96, 156, and 123 mm, respectively) exhibited the most pronounced damage. Ridge formation commenced in almost all specimens during the third cycle, with the initial appearance occurring between 150 and 230 mm from the point where the column contacted the stub. The region with the most substantial damage was concentrated between 126 and 250 mm from the stub face. The test outcomes underscored the prevalence of shear effects on the specimens.

Table 3. Values of displacement and ductility index

Column	δ_Y (mm)	δ_U (mm)	λ_δ	% increase
CC	6.9	54.5	7.89	-
PWC	7.14	75	10.5	33
FWC	4.7	72	15.3	93

8.2 Ductility

The ductility of structural elements is a measure of their capacity for plastic deformation. A higher ductility index signifies an increased capability for both energy dissipation and plastic deformation (Paulay and Priestley, 1992; Park, 1989). The displacement ductility index is expressed by the following equation (Park, 1989).

$$\lambda_\delta = \delta_U / \delta_Y \quad \ldots\ldots\ldots (1)$$

In the equation, δ_U and δ_Y represent lateral displacements at the ultimate and yield points, respectively. Determining the yield point displacement in reinforced concrete structures involves a subjective assessment due to the nonlinear behavior of materials and members exhibiting varied yielding under different loading conditions. These enhancements indicate the effectiveness of GFRP in fortifying columns against seismic forces, reducing vulnerability to damage and enhancing overall structural resilience. Such findings underscore the role of GFRP as a valuable retrofitting material for improving the seismic performance of existing RC structures, promoting safer and more resilient infrastructure. However, the effectiveness of ductility enhancement strategies alone varies depending on structural configuration and seismic risk. In this study, the lateral displacement at the yield point was defined using the idealized bilinear curves of columns. These curves were based on reduced stiffness, calculated at the secant stiffness, either at 75% of the lateral strength or at the first yield, whichever was lower (Priestley and Park, 1987). Ductility enhancement alone showed varied effectiveness depending on structural conditions and seismic risks. Thus, GFRP emerges as a comprehensive retrofitting solution for enhancing structural performance in seismic events, effectively addressing multiple aspects of resilience. The displacement and ductility index values are presented in Table 3.

8.3 Energy Absorption

The process of energy absorption is essential for reducing the seismic force acting on columns. When examining the hysteretic behavior of RC structural components, a key characteristic to consider is their energy dissipation capacity. In the event of an earthquake, RC structural elements lacking sufficient energy dissipation capacity are susceptible to significant displacements and may even collapse as a result of the cumulative energy lost from minor deformations. The energy dissipation inside the cycle is represented by the area enclosed within the hysteretic loops of the load-displacement curve for the specimens. Fig. 7 shows the absorbed energy content of the specimens. Hysteretic loops open in response to additional load, causing the enclosed area to increase rapidly, thereby improving the capacity to dissipate energy. However, GFRP has a stronger impact on this factor. Retrofitting square RC columns with GFRP wraps results in substantial improvements in seismic performance compared to conventional, unreinforced columns. The retrofitting enhances lateral strength by 96%, significantly increases ductility (26.1% to 74.1% depending on comparison), and boosts energy absorption capacity by up to 130%. As seen in Table 4 and Fig. 8, the energy absorption value of the original specimens is increased by GFRP textiles.

Table 4. Cumulative energy absorption

Column	Energy absorption (Nmm)	Increase %
CC	20602.6	-
PWC	40528.1	96
FWC	47634.5	130

8.4 Stiffness

The deformation capacity of the column is determined by the circular stiffness of the tested specimens. Stiffness is calculated from the hysteresis behavior of columns. The value of stiffness is given by the change of lateral loads at the n^{th} cycle in the positive and negative direction at unloading points and by the displacement difference, as given by the following equation (Mayes and Clough, 1975).

$$K_i = (P^+_{max} - P^-_{max})/(\delta^+_{max} - \delta^-_{max}) \quad \ldots\ldots (2)$$

where P^+_{max} and P^-_{max} indicate the maximum lateral strength in the positive and negative directions of push and pull, respectively. δ^+_{max} and δ^-_{max} indicate the maximum displacements in the positive and negative directions of push and pull, respectively. As the number

of cycles increase, the stiffness of the columns gradually decreases. The stiffness of the columns strengthened with GFRP also reduces with an increase in the number of cycles. The transverse rebars improve the core concrete strength and increase shear strength. The use of GFRP fibers enhances the strength of transverse reinforcement and helps to prevent early buckling of longitudinal reinforcement.

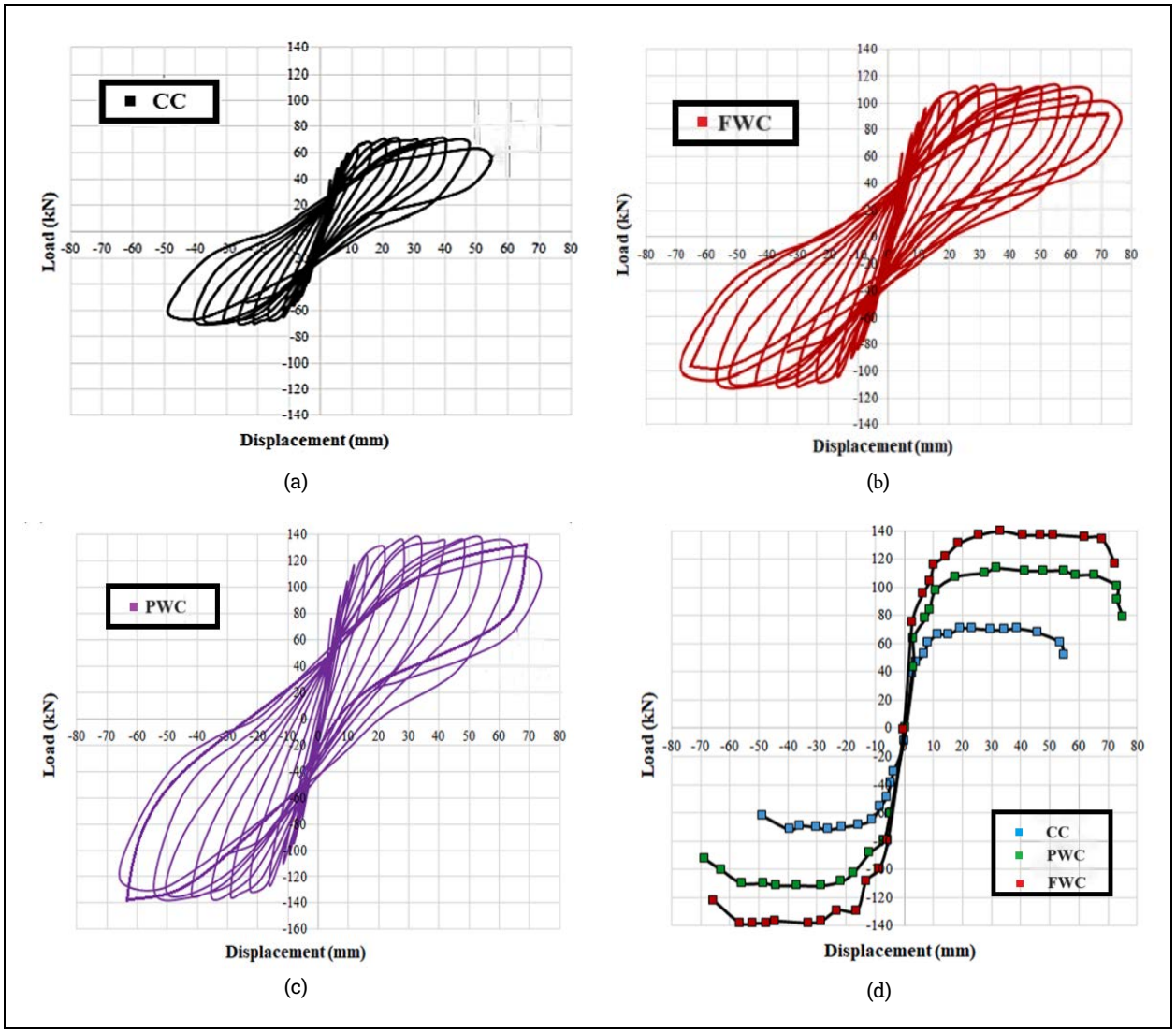

Fig. 8: (a, b, c) shows the hysteresis curve of specimens, and (d) shows the load-displacement curve of columns

9. CONCLUSION

In this investigation, the seismic performance of square RC columns subjected to retrofitting with GFRP was scrutinized and compared with that of conventional RC columns. To assess the performance of the RC specimens regarding lateral strength, ductility, and energy absorption, they were enveloped with GFRP wraps for comparison with reinforced columns lacking external retrofitting. The utilization of GFRP in retrofitting significantly enhances the lateral strength of retrofitted columns under lateral cyclic loading. The test results unequivocally demonstrate a 96% increase in the lateral strength of the retrofitted specimen compared to the conventional column. The ductility of the retrofitted specimens showed a significant increase under lateral cyclic loading. The column retrofitted with GFRP exhibited an increased ductility of 26.1% to 74.1% compared to the column without GFRP retrofitting. The specimens wrapped with GFRP showed an improved energy absorption capacity of about 96% and 130% compared to unwrapped column.

REFERENCES

ACI PRC-374.2-13 (2013), Guide for testing reinforced concrete structural elements under slowly applied simulated seismic loads, American Concrete Institute (2013).

Adam, J. M., Buitrago, M., Bertolesi, E., Sagaseta, J. and Moragues, J. J., Dynamic performance of a real-scale reinforced concrete building test under a corner-column failure scenario, *Eng. Struct.*, 210, 110414 (2020). https://doi.org/10.1016/j.engstruct.2020.110414

Benzaid, R., Chikh, N. E. and Mesbah, H., Study of the compressive behavior of short concrete columns confined by fiber reinforced composite, *Arab. J. Sci. Eng.*, 34(1B), 15-26 (2009).

Desprez, C., Mazars, J., Kotronis, P. and Paultre, P., Damage model for FRP-confined concrete columns under cyclic loading, *Eng. Struct.*, 48, 519-531 (2013). https://doi.org/10.1016/j.engstruct.2012.09.019

Galal, K., Arafa, A. and Ghobarah, A., Retrofit of RC square short columns, *Eng. Struct.*, 27(5), 801-813 (2005). https://doi.org/10.1016/j.engstruct.2005.01.003

Haroun, M. A., Feng, M., Elsanadedy, H. and Mosallam, A., Composite jackets for the seismic retrofit and repair of bridge columns, *In Proc., 7th US National Conf. on Earthquake Engineering*, 10 (2002).

Hua, J., Eberhard, M. O., Lowes, L. N. and Gu, X., Modes, mechanisms, and likelihood of seismic shear failure in rectangular reinforced concrete columns, *J. Struct. Eng.*, 145(10), 04019096 (2019). https://doi.org/10.1061/(ASCE)ST.1943-541X.0002365

Iacobucci, R. D., Sheikh, S. A. and Bayrak, O., Retrofit of square concrete columns with carbon fiber-reinforced polymer for seismic resistance, *J. Struct.*, 100(6), 785-794 (2003).

Institute, S. E., Minimum design loads for buildings and other structures, *American Society of Civil* Engineers (2006). https://doi.org/10.1061/9780784412916

Kiakojouri, F., De Biagi, V., Chiaia, B. and Sheidaii, M. R., Progressive collapse of framed building structures: Current knowledge and future prospects, *Eng. Struct.*, 206, 110061 (2020). https://doi.org/10.1016/j.engstruct.2019.110061

Kumutha, R., Vaidyanathan, R. and Palanichamy, M. S., Behaviour of reinforced concrete rectangular columns strengthened using GFRP, *Cem. Concr. Compos.*, 29(8), 609-615 (2007). https://doi.org/10.1016/j.cemconcomp.2007.03.009

Ma, Y. and Gong, J. X., Probability identification of seismic failure modes of reinforced concrete columns based on experimental observations, *J. Earthq. Eng.*, 22(10), 1881-1899 (2018). https://doi.org/10.1080/13632469.2017.1309603

Mayes, R. L. and Clough, R. W., State-of-the-art in seismic shear strength of masonry: an evaluation and review, University of California (1975).

Murray, J. A. and Sasani, M., Seismic shear-axial failure of reinforced concrete columns vs. system level structural collapse, *Eng. Fail. Anal.*, 32, 382-401 (2013). https://doi.org/10.1016/j.engfailanal.2013.04.014

Park, R., Evaluation of ductility of structures and structural assemblages from laboratory testing, *Bull. N.Z. Soc. Earthq. Eng.*, 22(3), 155-166 (1989). https://doi.org/10.5459/bnzsee.22.3.155-166

Paulay, T. and Priestley, M. N., Seismic design of reinforced concrete and masonry buildings, New York: Wiley, 768 (1992).

Priestley, M. J. and Park, R., Strength and ductility of concrete bridge columns under seismic loading, *J. Struct.*, 84(1), 61-76 (1987). https://doi.org/10.14359/2800

Promis, G., Ferrier, E. and Hamelin, P., Effect of external FRP retrofitting on reinforced concrete short columns for seismic strengthening, *Compos. Struct.*, 88(3), 367-379 (2009). https://doi.org/10.1016/j.compstruct.2008.04.019

Sharma, S. S., Dave, U. V. and Solanki, H., FRP wrapping for RC columns with varying corner radii, *Procedia Eng.*, 51, 220-229 (2013). https://doi.org/10.1016/j.proeng.2013.01.031

Shin, D. H. and Kim, H. J., Cyclic response of rectangular RC columns retrofitted by hybrid FRP sheets, *Struct.*, 28, 697-712 (2020). https://doi.org/10.1016/j.istruc.2020.09.016

Theiss, A., The impact of beam-column joint damage on the response of an older reinforced concrete frame building (Doctoral dissertation, MS Thesis, CE & E Dept., University of Washington) (2005).

Watson, S. and Park, R., Simulated seismic load tests on reinforced concrete columns, *J. Struct. Eng.*, 120(6), 1825-1849 (1994). https://doi.org/10.1061/(ASCE)0733-9445(1994)120:6(1825)

Ye, L., Yue, Q., Zhao, S. and Li, Q., Shear strength of reinforced concrete columns strengthened with carbon-fiber-reinforced plastic sheet, *J. Struct. Eng.*, 128(12), 1527-1534 (2002). https://doi.org/10.1061/(ASCE)0733-9445(2002)128:12(1527)

Yoddumrong, P., Rodsin, K. and Katawaethwarag, S., Experimental study on compressive behavior of low and normal strength concrete confined by low-cost glass fiber reinforced polymers (GFRP), *In IEEE 3rd Int. Conf. Eng. Sci. Innov. Technol. Proc., (ESIT)*, 1-4 (2018). https://doi.org/10.1109/ESIT.2018.8665331

Yoddumrong, P., Rodsin, K. and Katawaethwarag, S., Seismic strengthening of low-strength RC concrete columns using low-cost glass fiber reinforced polymers (GFRPs), *Case Stud. Constr. Mater.*, 13, e00383 (2020). https://doi.org/10.1016/j.cscm.2020.e00383

Zhu, L., Elwood, K. J. and Haukaas, T., Classification and seismic safety evaluation of existing reinforced concrete columns, *J. Struct. Eng.*, 133(9), 1316-1330 (2007). https://doi.org/10.1061/(ASCE)0733-9445(2007)133:9(1316)